PREDICTION OF NONUNIFORM INLET TEMPERATURE EFFECTS ON VANE AND ROTOR HEAT TRANSFER

R. J. Boyle
NASA Lewis Research Center
Cleveland, OH 44135

P. W. Giel
NYMA, Inc.
Cleveland, OH 44135

ABSTRACT

The effects of nonuniform combustor exit temperature profiles on vane and rotor heat transfer were determined using a steady-state three-dimensional Navier-Stokes analysis. Both radial and tangential nonuniform temperature profiles were individually considered. Comparisons are made with experimental data for the effects of a radial temperature nonuniformity on rotor heat transfer. There was a decrease in stator heat load, and an increase in rotor heat load for a radial temperature distribution typically seen at the combustor exit. Tangential variations in stator inlet temperature produced significant variations in stator heat load, and resulted in average rotor heat load greater than for the uniform inlet temperature case. Rotor heat load was also calculated for different stator wake locations. Accounting for the stator wake position at the rotor inlet gave a greater average rotor heat load than that obtained by averaging the stator exit flow field in the tangential direction. The increase was most notable on the rotor pressure surface.

Nomenclature

c	-	True chord
c_x	-	Axial chord
h	-	Heat transfer coefficient
k	-	Thermal conductivity
Nu	-	Nusselt number
q	-	Heat flux
r	-	Radius
St	-	Stanton number
s	-	Surface distance
T	-	Temperature
γ	-	Specific heat ratio
θ	-	Ratio of temperature differences
Subscripts		
HUB	-	Hub
IN	-	Gas inlet
MAX	-	Maximum
MIN	-	Minimum
NU	-	Nonuniform
PROFILE	-	Nonuniform profile - Radial or Tangential
RANGE	-	Range of values
REL	-	Relative to uniform
r	-	Radial
TIP	-	Casing
WALL	-	Surface
Superscripts		
$'$	-	Absolute total condition
$''$	-	Rotor relative total condition
$\bar{}$	-	Average

INTRODUCTION

In actual gas turbine engine operation the temperature field at the combustor exit is not uniform. To limit combustor metal temperatures the midspan temperature is significantly higher than the average gas temperature. Gas temperature variations in the blade-to-blade direction also occur. These turbine inlet temperature variations affect the local heat load for both stator and rotor blades. Spanwise variations in temperature at the combustor exit were documented by Cox(1975), and Suo(1985). Pitchwise variations in combustor exit temperature can also be present. Crocker et al.(1994) presented data showing the pitchwise variation in temperature to be as large as the spanwise variation.

Several researchers have reported experimental and numerical studies of the changes in the turbine flow field resulting from nonuniform conditions at the stator inlet. Butler et al.(1986) showed experimentally that, when heated air was introduced near midspan at the stator inlet, segregation of the fluid occurred within the rotor passage. Cold fluid migrated towards the suction surface, and hot fluid migrated towards the pressure surface. Saxer and Giles(1990) presented an Euler analysis which led to the same conclusions as Butler et al.(1986) regarding the segregation of hot and cold fluid within the rotor passage. Heselhaus and Vogel(1995) used a three dimensional Navier-Stokes analysis to show that a radial temperature profile significantly lowered stator suction surface heat load in the region close to the endwall.

The flow and surface heat transfer for the rotor and to a lesser extent the stator are inherently unsteady. Generally, investigators have focused on obtaining the unsteady pressure distribution for a turbine stage. Jorgenson and Chima(1988), and Rao et al.(1992) presented the results of an unsteady analysis for the midspan pressure distribution of a turbine stage. Davis et al.(1996) presented results for a three dimensional Navier-Stokes computational analysis for the unsteady flow field for a multi-stage configuration. Takahashi and Ni(1991) compared their analysis of a hot streak on the flow distribution within a turbine with the experimental data of Butler et al.(1986).

Compared to surface pressures, predictions of heat transfer require significantly more iterations for convergence. Closer grid spacing near the surface are also required for heat transfer predictions. For these reasons unsteady Navier-Stokes predictions of surface heat transfer have been confined to the midspan region. Rao et al.(1992a) showed predictions and comparisons with experimental data for the midspan of a turbine stage. When a radially varying inlet temperature profile is present the flow field is even more three dimensional than for a uniform inlet profile. It was felt that a three-dimensional analyses was necessary, but that an unsteady analysis would require excessive CPU time. It was estimated that a three-dimensional unsteady analysis of surface heat transfer would require several hundred supercomputer CPU hours, even if the acceleration techniques proposed by Davis et al.(1996), and by Arnone and Pacciani(1996) were used. To determine the effects of variations in stator inlet temperature several cases would have to be examined. Because of the large CPU time requirements an unsteady analysis was not done. In the approach taken the stator flowfield was decoupled from the rotor. The stator was analyzed for a number of different inlet temperature profiles. The output for each case was then used as input for the rotor analysis. Generally, the flow field was not averaged in the tangential direction. This approach has some similarities to the one advocated by Dorney et al.(1996) in their analysis of unsteady turbomachinery flows. The approach used herein has the added simplification that the unsteadiness at the stator exit on the stator flow field was not considered.

The objective of this work is to quantify the variation in local heat load due to temperature variations at the stator inlet. It was determined that, especially for tangential variations in temperature, averaging the stator exit flow field for input to the rotor analysis would not adequately determine the effects of stator inlet temperature variations on the rotor heat transfer. A procedure was developed to maintain the stator exit flow field characteristics while calculating the rotor heat transfer. This procedure led to results which, in addition to determining the average rotor heat transfer, yielded the variation in rotor heat transfer due to the stator wake being at different rotor inlet locations.

Results are presented for the single stage turbine described by Shang et al.(1995). This turbine was a high specific work stage with an overall pressure ratio of 4.3. Both the stator and rotor exit Mach numbers were greater than one. Comparisons are shown with the data of Shang et al.(1995) for the effects of a radial temperature distribution on rotor heat transfer.

DESCRIPTION OF COMPUTATIONAL ANALYSIS

The analysis was done using the steady-state three-dimensional Navier-Stokes code, RVC3D, described by Chima(1991), and by Chima and Yokota(1988). Comparisons with experimental heat transfer data for both vanes and rotors using this code have been reported, (Boyle and Giel(1995), Boyle and Jackson(1995), and Boyle and Lucci(1996)). The reported results were for cases in which the inlet flow field was uniform in the tangential direction for both vanes and rotors. A steady-state analysis was used rather than a unsteady analysis because the focus of the work was to explore the effects of nonuniform temperatures at the stator inlet on both stator and rotor heat transfer. It was felt that the relative effects of temperature nonuniformities could be obtained without resorting to a three-dimensional unsteady Navier-Stokes analysis. The analysis was done considering one blade row at a time. The stator heat transfer was calculated assuming both uniform and nonuniform inlet total temperature profiles. Since the stator inlet Mach numbers were low, the differences between the inlet static and total temperature profiles were small. The radial profiles were parabolic in shape. The tangentially varying profiles were sinusoidal in shape, with a period equal to the pitch of the stator. A series of tangential profiles were considered, so that the peak temperature was positioned at different locations across the inlet to the computational domain of the stator. Both the radial and tangentially varying inlet temperature profiles were calculated to give the same average inlet total

temperature as the uniform inlet temperature baseline case. Uniform temperature boundary conditions were imposed on all solid surfaces.

The code RVC3D, (Chima(1991), and Chima and Yokota(1988)), utilizes a finite difference approach to solving the three-dimensional Navier-Stokes equations. A Runge-Kutta time marching approach with locally varying time steps is used to obtain a steady-state solution. Implicit residual smoothing is used to improve convergence. C-type grids were used, and along the outer boundary of the C grid periodicity was imposed. The inlet boundary conditions used were somewhat different for the stator and rotor. For stators the inlet freestream total pressure and temperature were specified, along with the inlet boundary layer thickness. The exit static pressure at the hub was specified. There was no swirl at the inlet, so that the tangential and radial velocities were zero. The axial velocity, and thus mass flow, was determined by the flow solution. After a solution was obtained for a specific set of stator boundary conditions, the resulting flow field was interpolated at a constant axial coordinate. This was chosen to be $0.2c_x$ behind the stator. The results from the interpolation became the inlet flow conditions for the rotor. The flow variables at the stator exit were geometrically scaled, and used as input for the rotor heat transfer analysis. The total temperature and all of the other flow variables were unchanged, but their tangential coordinates were reduced by the ratio of the stator-to-rotor blade count. The rotor hub exit pressure was set based on specified conditions. The only inlet velocity that was allowed to change as the solution progressed was the axial velocity. The overall mass flow changed very little from what was initially specified during the course of obtaining the rotor solution.

Both Ameri and Arnone(1994), and Chima(1996) showed heat transfer comparisons using algebraic and two-equation turbulence models. They showed no significant improvement in heat transfer prediction for the two-equation turbulence models compared to the algebraic turbulence model. However, the two-equation models may require nearly twice the CPU time to converge. Therefore, an algebraic turbulence model was used for the predictions. It is the one described by Chima et al.(1993). A few predictions were also made using the Baldwin-Lomax(1978) turbulence model. While the choice of turbulence model did affect the heat transfer level somewhat, the relative effects of a nonuniform inlet total temperature were not affected by the choice of turbulence model. Fully turbulent flow was assumed for two primary reasons. First, in actual applications the flow is likely to be turbulent at or near the leading edge. The high level of turbulence at the combustor exit is likely to give transition near the leading edge. If there is film cooling at the leading edge, the boundary layers will be turbulent. The second reason for assuming fully turbulent flow was to help

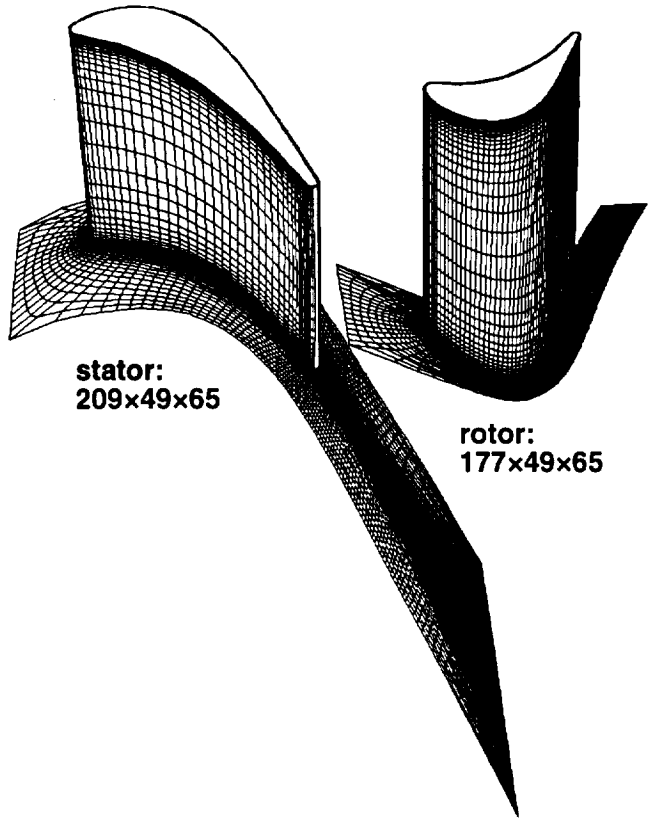

Fig. 1 – Stage geometry and grid.

clarify the effects of inlet temperature nonuniformities. If transition were allowed to occur along the vane surfaces, the start and end of transition would be affected by the local freestream temperature. Thus some of the indicated change in heat transfer due to temperature nonuniformities would be due to changes in the transition location, which could also be brought about by changes in other factors such as turbulence intensity.

C-type grids were generated using the code described by Arnone et al.(1992). In the near wall region grid lines were embedded within a coarse grid. The coarse grid was generated using Sorenson's(1980) technique. Different size grids were used, the smallest being $177 \times 49 \times 65$. In order to accurately represent the nonuniform conditions at the stator or rotor inlet, 16 grid cells were used at the inlet in the blade-to-blade direction. Figure 1 illustrates the grids used for both the stator and rotor. The RVC3D code was modified to accept non-matching grid lines along the cut line from the blade trailing edge stagnation point to the exit of the computational domain. This facilitated having sixteen grid cells at the inlet, without excessive shearing of the grid. The exit was at least $0.5c_x$ beyond the trailing edge.

Computations were performed using the Cray C-90 at the NAS facility at the NASA Ames Research Center. The code was highly vectorized. The average CPU time per grid

point per time cycle was 6×10^{-6} seconds. Heat transfer results typically takes two-to-three times as many iterations to converge than do surface pressures. The nonuniform inlet cases took longer to converge than the uniform inlet cases. Generally the cases were converged in two CPU hours, and were run up to an additional hour to assure convergence. Based on an examination of the results from a large number of cases, it is estimated that surface heat transfer differences between cases of less than 10% should not be considered significant.

DISCUSSION of RESULTS

Vane surface heat transfer will be presented first. Results will be shown for a base case of a uniform inlet temperature profile, a radially varying inlet temperature profile, and four tangentially varying inlet temperature profiles. Each of these six stator inlet profiles resulted in different flow conditions at the stator exit. These flow conditions were then used to determine the effects of variations in stator inlet temperature distributions on rotor surface heat transfer. Comparisons will be shown with the experimental data of Shang et al.(1995) for the effect of a radial temperature variation on rotor surface heat transfer. The Reynolds number based on stator true chord and isentropic exit conditions was 2.7×10^6. The stator exit Mach number was 1.22, and $\gamma = 1.28$. The stage total pressure ratio was 4.3.

Stator heat transfer

Figure 2 shows the vane, hub, and casing Stanton numbers for the the uniform inlet temperature baseline case. Heat transfer is shown in terms of Stanton number, with the reference density and velocity based on the average conditions at the exit of the vane row. The vane heat transfer is shown for an unwrapped surface. The non-rectangular shape of the contour plot boundary shows the endwall converging, with most of the convergence occurring near the leading edge. The Stanton number is relatively high in the leading edge region compared to what would be expected from assuming laminar flow because the analysis assumed fully turbulent flow. The vane heat transfer shows little spanwise variation. The peak Stanton number on the pressure surface occurs close to the trailing edge, and approaches the same level as the peak suction surface Stanton number, which occurs closer to the leading edge. The hub and casing heat transfer distributions are similar. The peak hub heat transfer is in a region close to the pressure surface, somewhat upstream of the throat. The hub heat transfer shows some influence of the passage shock emanating from the pressure side trailing edge. The effects are somewhat diffused before reaching the suction surface. The tip exit is subsonic, and the casing heat transfer shows no evidence of a passage shock.

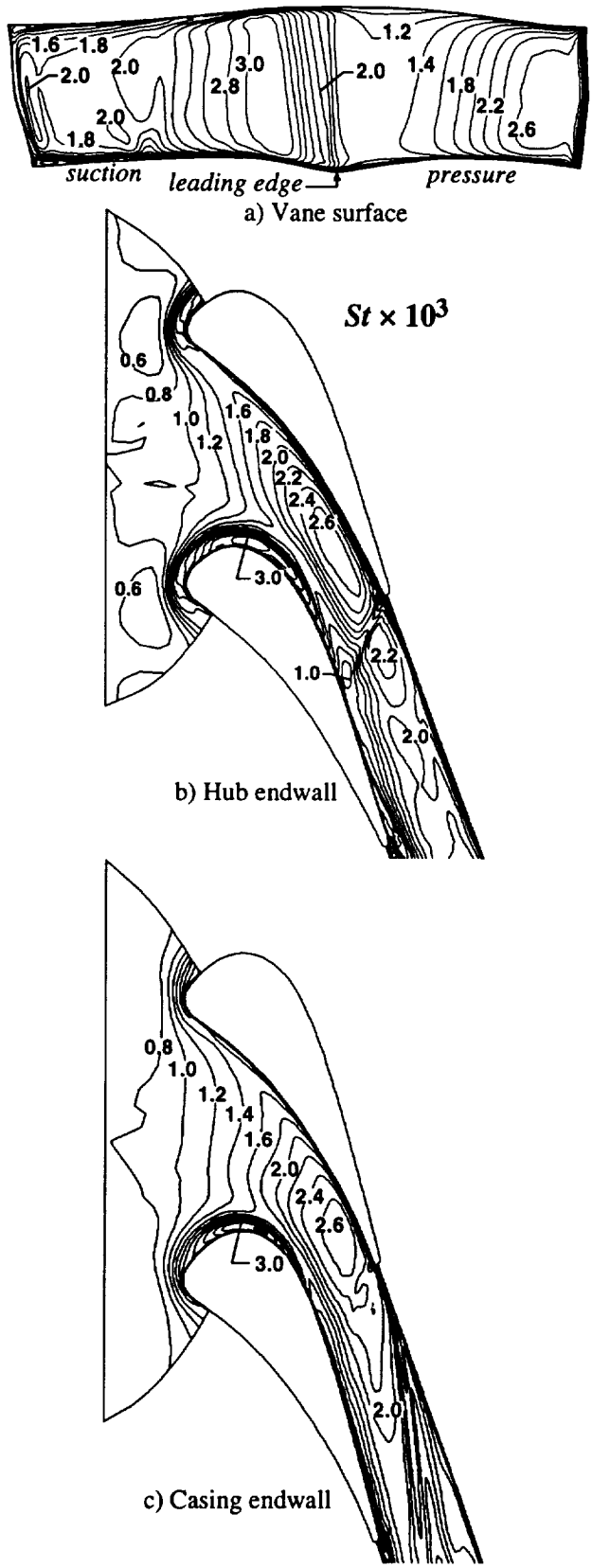

Fig. 2 Stanton number distribution for stator of transonic turbine.

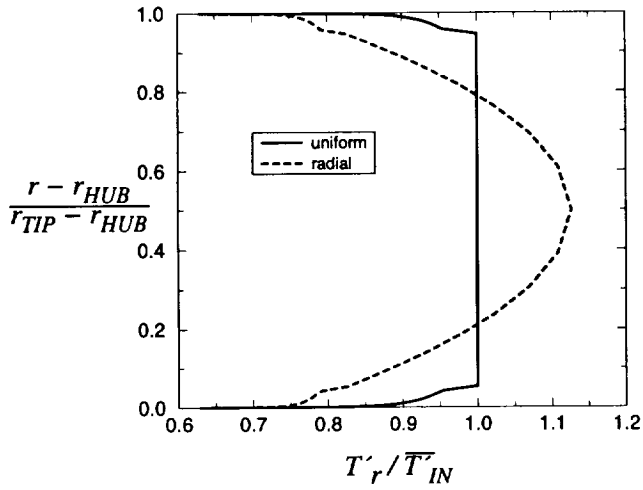

Fig. 3 – Stator inlet total temperature distributions for transonic turbine.

A comparison of normalized total temperature profiles for the uniform and radially varying cases is shown in figure 3. The average normalized inlet total temperature, $\overline{T}'_{\mathrm{IN}}$, is the same for both profiles. The hub and casing boundary layer thicknesses are 5% of the span. At the surface the gas and wall temperatures are equal, $T_{\mathrm{WALL}}/\overline{T}'_{\mathrm{IN}} = 0.63$. Outside the endwall boundary layers the normalized total pressure is 1. At each endwall surface the total pressure equals the static pressure. The ratio of static-to-freestream total pressure is 0.986.

Figure 4 compares the effects of the radial inlet profile on vane and hub heat transfer in terms of the relative heat transfer. Where:

$$h_{\mathrm{REL}} = 100 \times (h_{\mathrm{PROFILE}} - h_{\mathrm{UNIFORM}})/h_{\mathrm{UNIFORM}}$$

Negative values for h_{REL} correspond to heat loads lower than for the uniform inlet temperature case.

Since the heat transfer coefficients were calculated from $h = q_{\mathrm{WALL}}/(\overline{T}'_{\mathrm{IN}} - T_{\mathrm{WALL}})$, and $\overline{T}'_{\mathrm{IN}} - T_{\mathrm{WALL}}$ is the same for both profiles, changes in heat transfer coefficient are equivalent to changes in heat flux at the surface. The midspan driving potential for the radial temperature profile, $T'_{\mathrm{IN}} - T_{\mathrm{WALL}}$, is greater than the driving potential for the uniform temperature profile by a factor of 1.34. The ratio of a nonuniform maximum thermal driving potential to the uniform midspan potential is given by:

$$\theta_{\mathrm{NU}} = \frac{(T'_{\mathrm{IN-MAX}} - T_{\mathrm{WALL}})_{\mathrm{NONUNIFORM}}}{(T'_{\mathrm{IN}} - T_{\mathrm{WALL}})_{\mathrm{UNIFORM-MIDSPAN}}}$$

If the radial nonuniformity did not influence the flow field, the midspan heat transfer should increase by the same amount as θ. The midspan heat transfer does not increase

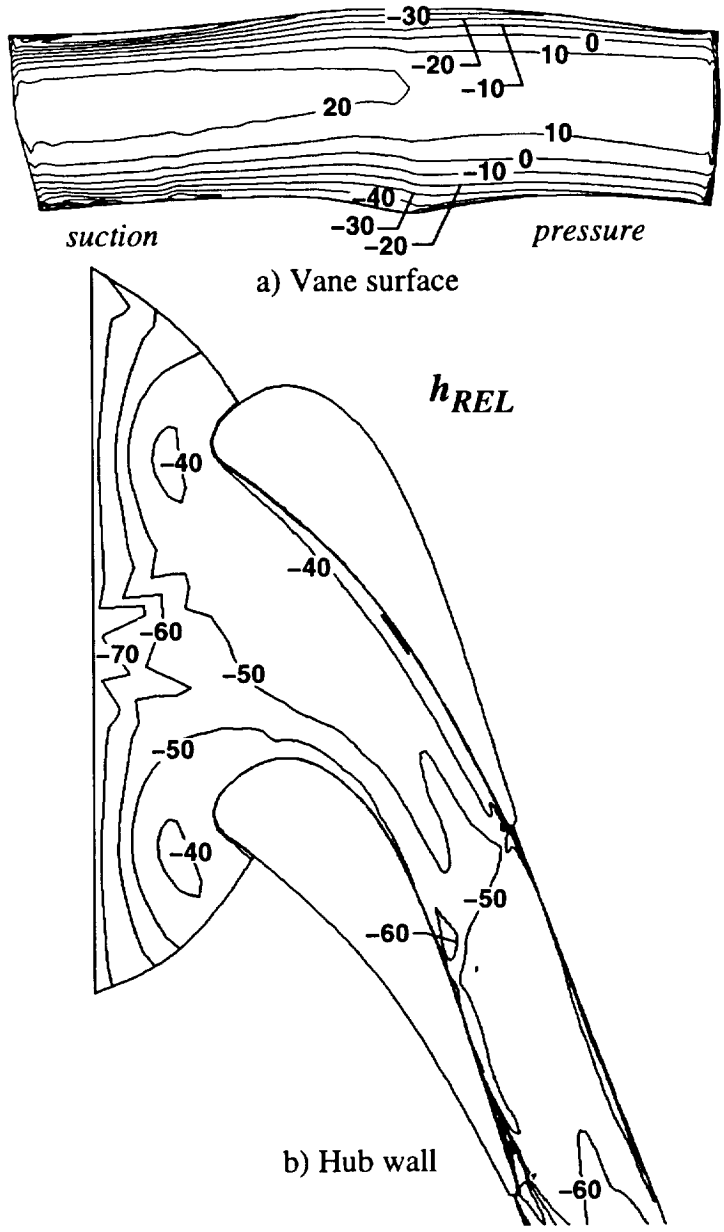

Fig. 4 Heat transfer distribution – radial profile relative to uniform profile

by this ratio, indicating that redistribution of the stator flow field affected midspan heat transfer. The maximum increase in midspan heat transfer was only about half of the increase in driving potential, and occurred along the suction surface. The pressure surface midspan heat transfer shows only a very small heat transfer increase due to a radial temperature profile. Away from the midspan the reduced heat transfer with a radial temperature profile is expected. Near the endwalls the inlet gas temperature is less than the average temperature.

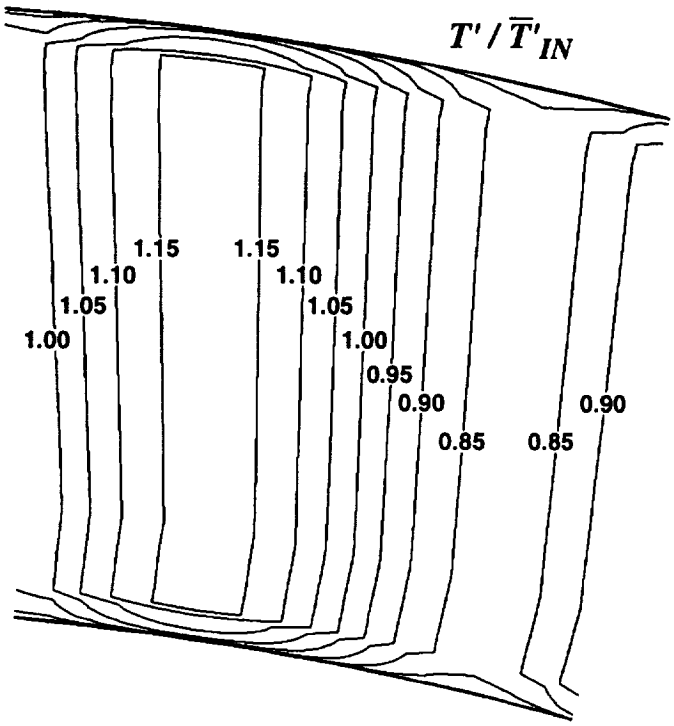

Fig. 5 Tangentially varying stator inlet temperature profile.

Analysis of the effects of radial temperature distribution on vane surface heat transfer for three other stator configurations showed similar trends to that seen in figure 4. The increase in midspan suction surface heat transfer was less than the increase in θ, and the increase in midspan pressure surface heat transfer was very small. The less than anticipated rise in midspan heat load with a radial temperature profile was investigated in detail. The choice of turbulence model did not cause the lower than expected heat load. Cases were run where the transition was allowed to occur according to the transition criterion of Mayle(1991). Surface heat transfer was calculated for both uniform and radial profile cases using this transition criterion. For these cases the flow in the leading edge region was laminar. The relative heat transfer in the midspan leading edge region was similar to the fully turbulent analysis. Analysis of the flow fields for the two inlet temperature profiles indicated that the lower than expected heat transfer was due to redistribution of the flow in the presence of the inlet radial temperature profile. For these annular cascades there is greater blockage near the hub compared to midspan. Even for the uniform inlet temperature case there are radially outward velocities at midspan. The flow distributions were examined along midspan grid lines emanating from the vane leading edge. When a radial temperature profile was present the radial velocities were significantly greater. In the vane region there was greater transport of fluid from the hub past the midspan region. For the radial temperature profile the gas temperature close to the hub was colder than for the uniform temperature profile. At midspan, colder fluid from the hub region lowered the temperature of the fluid near the leading edge. This resulted in the lower than expected heat transfer. A further indication that radial redistribution of the flow caused lower than expected heat load came from the spanwise average heat transfer. In the leading edge region the spanwise average heat transfer for the radial inlet profile case was within 1% of the spanwise average for the uniform inlet case.

Figure 4b shows the stator hub endwall relative heat transfer. Since the inlet temperature profile looks somewhat like a very thick thermal boundary layer, it is not surprising that endwall heat transfer is lower for a radial temperature profile. For most of the passage region the decrease is between 40 and 50%. This decrease is somewhat greater than the increase in midspan driving potential with the radial temperature gradient. Thus a 1% increase in θ results in nearly a 1.3% decrease in endwall heat load. It is expected that this ratio would be somewhat affected by the shape of the inlet radial temperature distribution. The relative decrease is lowest for a small region just in front of the leading edge. This is the result of the horseshoe vortex convecting fluid with a higher than average temperature towards the endwall. Although not shown, the results for the casing endwall were very similar to the hub endwall heat transfer. Overall, the surface heat transfer is lower with a radial temperature gradient than with a uniform inlet temperature.

Figure 5 shows the temperature profile used to determine the effects of a tangentially varying inlet temperature nonuniformity. The temperature distribution is periodic, and again the average inlet temperature is the same as the uniform inlet case. The maximum value for $T'/\overline{T}_{\rm IN}$ of 1.17 corresponds to $\theta = 1.46$. The midspan thermal driving potential, $T'_{\rm IN} - T_{\rm WALL}$, varies between 54% and 146% of the uniform inlet midspan driving potential, giving a range of nearly 90% in the midspan value. The tangential location of the maximum temperature was varied by rotating the profile in the tangential direction. Four cases were run, with the location of the maximum temperature moved a quarter of the period in each case.

It is unlikely that the pitch of an actual combustor exit profile will equal a vane pitch, Crocker et al.(1994). Therefore, the heat transfer distribution for a particular vane is unlikely to be determined by the analysis for a particular combustor exit pitchwise total temperature distribution. What is of interest, however, are comparisons of the averaged heat transfer distribution and the range of heat transfer expected from the tangential nonuniformity. Figure 6 shows a comparison of the heat transfer distribution obtained by averaging at each surface location the results from the four total inlet temperature distributions. Relative heat transfer

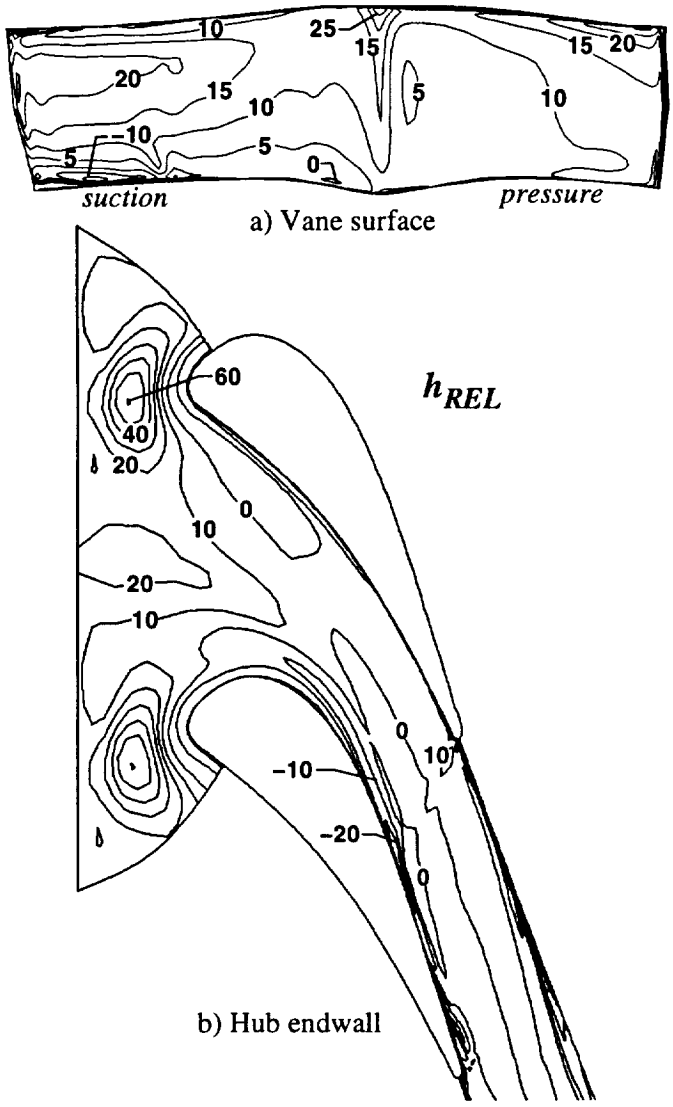

Fig. 6 Heat transfer distribution – average of four tangential locations relative to uniform profile.

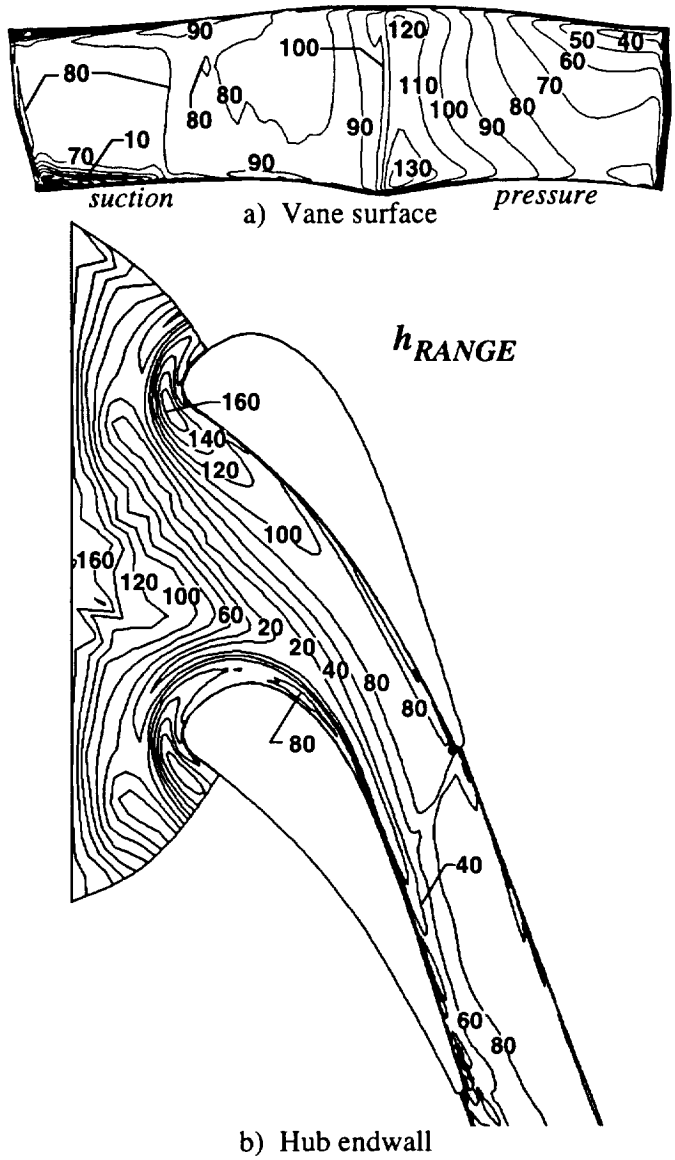

Fig. 7 Range in heat transfer resulting from four different pitchwise positions of tangentially varying inlet temperature profile.

rates are shown using the uniform inlet temperature case as the baseline. For the pressure surface there is little difference between the uniform inlet temperature profile and the average of the four tangential profiles. There is an increase of more than 20% in heat load for much of the suction surface above midspan for the average of the nonuniform inlet temperature cases. The pitchwise and radial variations in inlet total temperature produced similar effects for the vane surface heat transfer.

Hub heat transfer results are somewhat different from the vane surface results. Comparing the average of the nonuniform to uniform inlet temperature results shows an increase in average hub surface heat transfer for the forward part of the passage. There is heat transfer decrease for the rearward part of the passage. Figure 6 shows a large increase in the relative heat transfer as a result of tangentially nonuniform temperatures in the region just in front of the vane. These results are similar to those shown in figure 4 for the radial nonuniformity, but the peak is further in front of the leading edge. The increase in average heat transfer of up to 60% occurring in front of the leading edge may be somewhat misleading. In this region, as shown in figure 2, the base case has low heat transfer. Within the stator passage the change in h_{REL} are on the same order as θ (1.46).

The range of surface heat transfer resulting from the different pitchwise locations of the maximum temperature is given in figure 7. The range in heat transfer is given by:

$$h_{\mathrm{RANGE}} = 100 \times \frac{h_{\mathrm{MAX}} - h_{\mathrm{MIN}}}{\overline{h}}$$

At each surface point $\overline{h}$ is the mean of the values determining the range.

Much of the suction surface shows that the range in heat transfer is approximately 70 to 80%. This closely approximates the 90% range in the inlet midspan driving potential. A 1% variation in tangential driving potential results in nearly a 1% variation in suction surface heat load. The average range in pressure surface heat transfer is about the same as the suction surface average. However, locally the maximum range is 130%. At this location a 1% variation in inlet driving potential results in nearly 1.5% variation in heat load. A vane placed so as to experience the hottest tangential temperatures is expected to have a heat load increase at least as great as the value of θ for the combustor tangential nonuniformity. On the hub endwall, only in the leading edge region does the variation in heat load driving potential exceed the variation in driving potential. For the rest of the endwall the variation is somewhat less. Wherever $h_{\mathrm{RANGE}} > 2 \times (\theta - 1)$, a vane passage placed so as to experience the hottest tangential temperature is expected to have a heat load increase greater than θ.

Figure 8 shows total temperature distributions at $0.20c_x$ behind the vane for the six cases considered. The suction surface is to the right of the wake centerline, and the pressure surface is to the left. Because the stator is cooled, the minimum temperature location shows the wake centerline position. The uniform inlet temperature case has a total temperature ratio less than 0.96 for about 10% of the passage width. Consequently, the driving potential is lowered by more than 9% of the average over the entire plane for about 10% of the passage width. The endwall thermal boundary layers are thin. There is a low total temperature region near the hub and adjacent to the suction side of the wake. For the radial inlet temperature distribution the wake significantly affects the total temperature profile. On the pressure side of the wake hot fluid from the midspan region is brought closer to the hub by secondary flows. Overall, secondary flows are seen to significantly affect the total temperature profile.

The wake total temperature distributions for the four inlet profiles with tangential variations depend on the peak inlet temperature location. Figures 8c and 8e show that for the profile shown in figure 5, and the profile displaced 1/2 a pitch, the inlet tangential variation is generally observed at the exit. The profile displaced 3/4 of a pitch, and to a lesser extent 1/4 of a pitch, showed strongly distorted exit total temperature profiles. Overall, tangential variations in inlet temperature significantly affect exit temperatures.

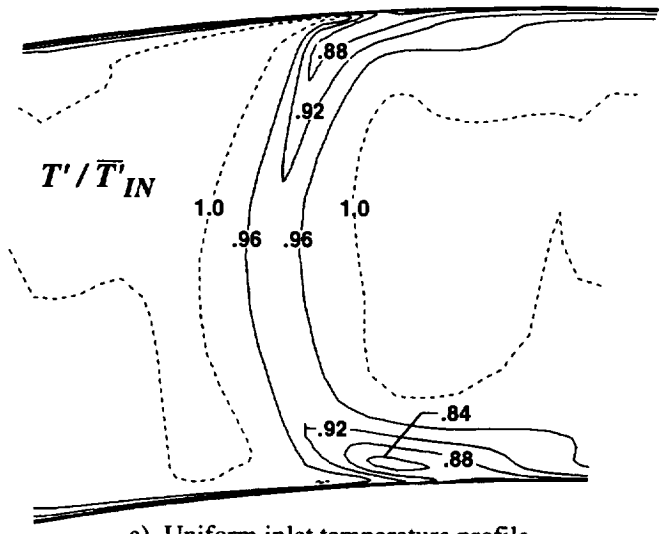

a) Uniform inlet temperature profile

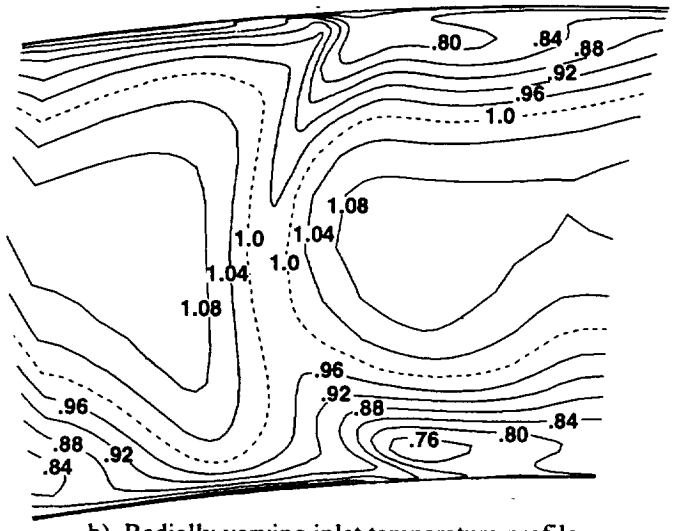

b) Radially varying inlet temperature profile

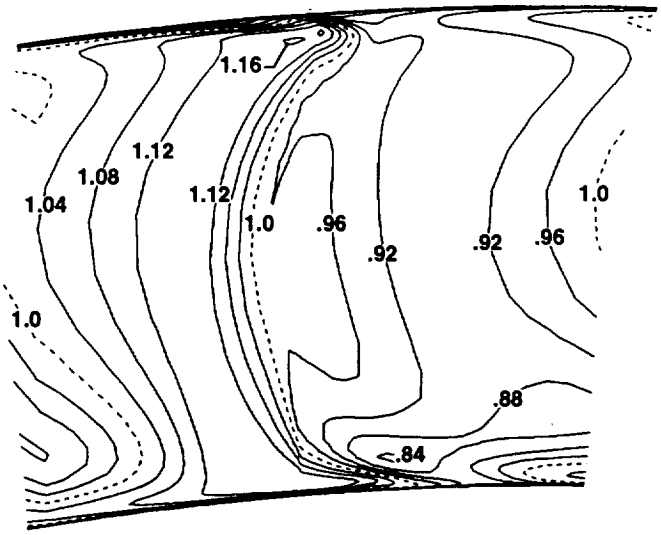

c) Tangentially varying profile – 0 shift

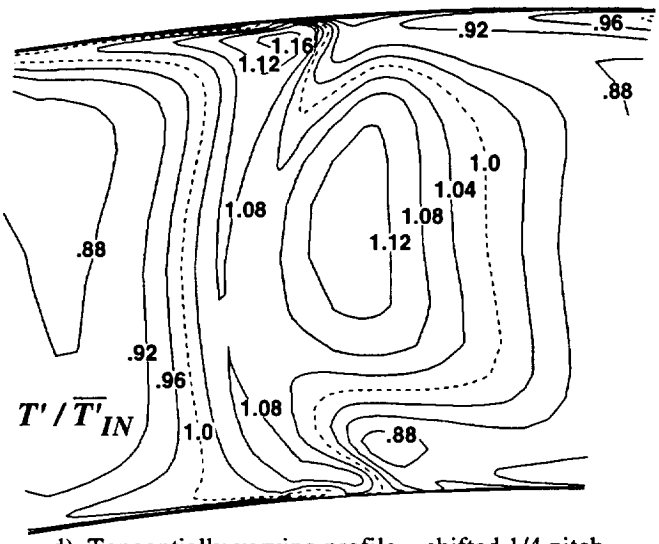

d) Tangentially varying profile – shifted 1/4 pitch

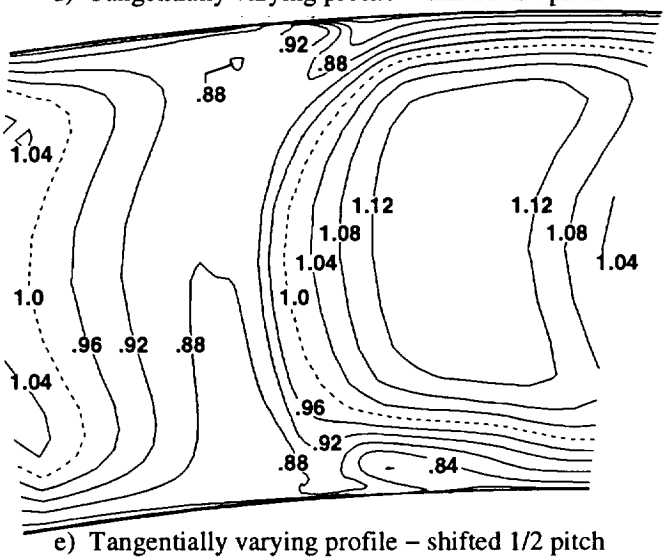

e) Tangentially varying profile – shifted 1/2 pitch

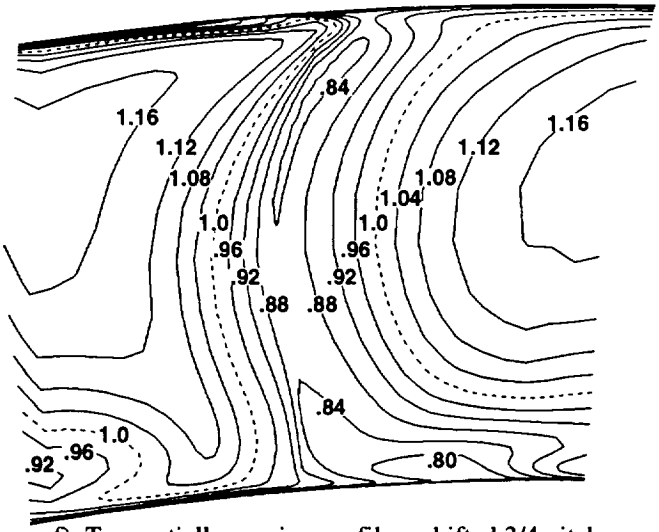

f) Tangentially varying profile – shifted 3/4 pitch

Fig. 8 Total temperature distribution $0.2c_x$ behind vane.

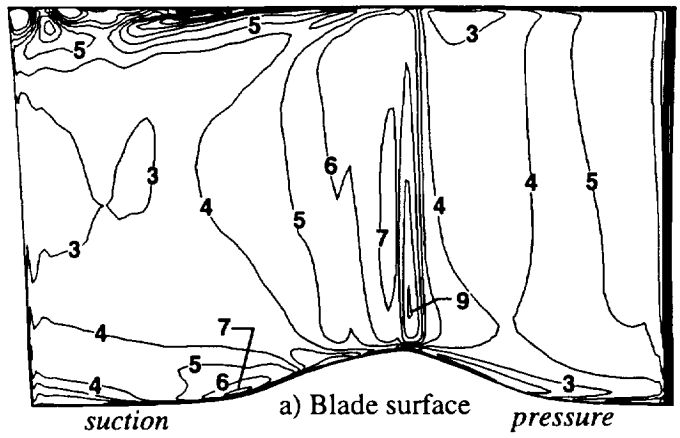

a) Blade surface

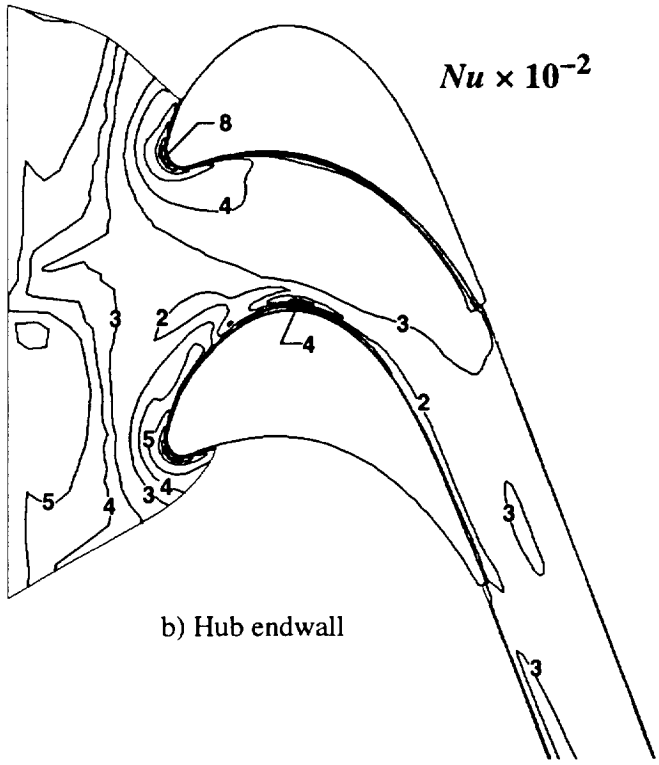

b) Hub endwall

Fig. 9 Nusselt number distribution for rotor of transonic turbine

Rotor heat transfer.

As mentioned previously, the coordinates of the total temperature profiles shown in figure 8 and other flow variables were geometrically scaled, and used as input for the rotor heat transfer analysis. For each of the six profiles shown in figure 8, the flow variable coordinates were rotated so that the wake location was at different rotor inlet tangential coordinates. Cases were run for rotations of 0, 1/3, and 2/3's of the rotor pitch for each of the six profiles. For each of the six profiles a fourth reference case was run in which the inlet profiles were averaged in the tangential direction.

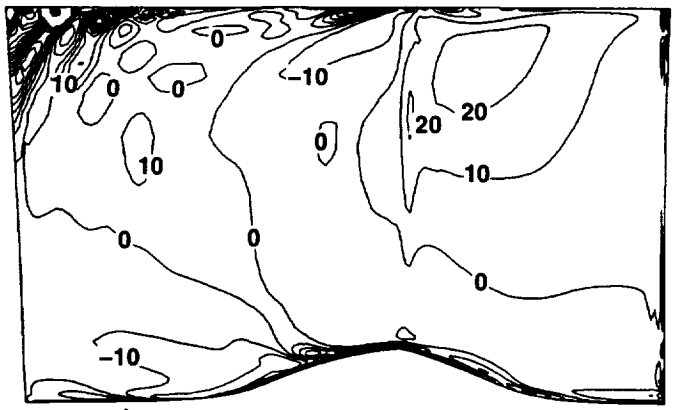

a) Blade surface – average heat transfer

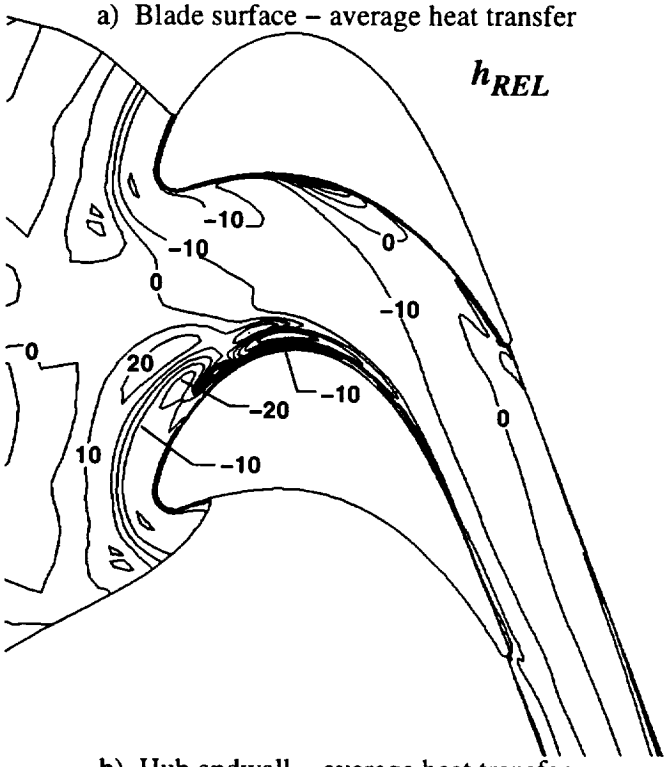

b) Hub endwall – average heat transfer

Figure 9 shows rotor heat transfer distributions on the blade surface and hub endwall for the uniform stator inlet temperature case. The flow variables at the stator exit were averaged in the tangential direction. Heat transfer rates are in terms of Nusselt number. Here $Nu = q_{WALL}c/k(\overline{T}_{IN})/(\overline{T}_{IN} - T_{WALL})$. The high leading edge region heat transfer results from assuming fully turbulent flow. There is little spanwise variation along the pressure surface. Along the suction surface there are very high gradients near the blade tip. The average tip region heat transfer is high due to clearance flow. The analysis was done for a 1% clearance gap. The high heat transfer values on the suction surface and the large spanwise gradients near the tip are consistent with results reported by Ameri and Steinthorsson(1995) using a different analysis. Calculations with zero clearance showed much smaller gradients near the tip of the rotor.

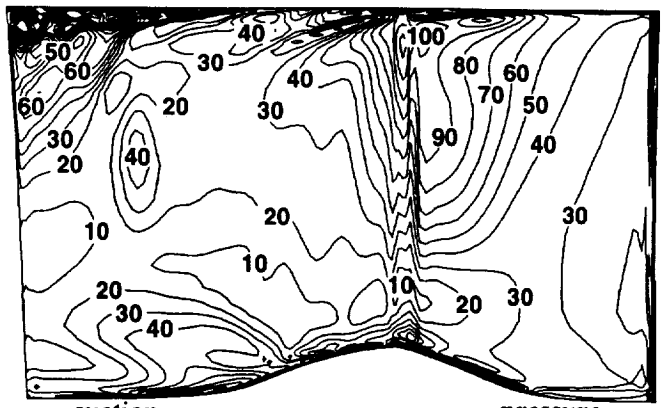

c) Blade surface – range in heat transfer

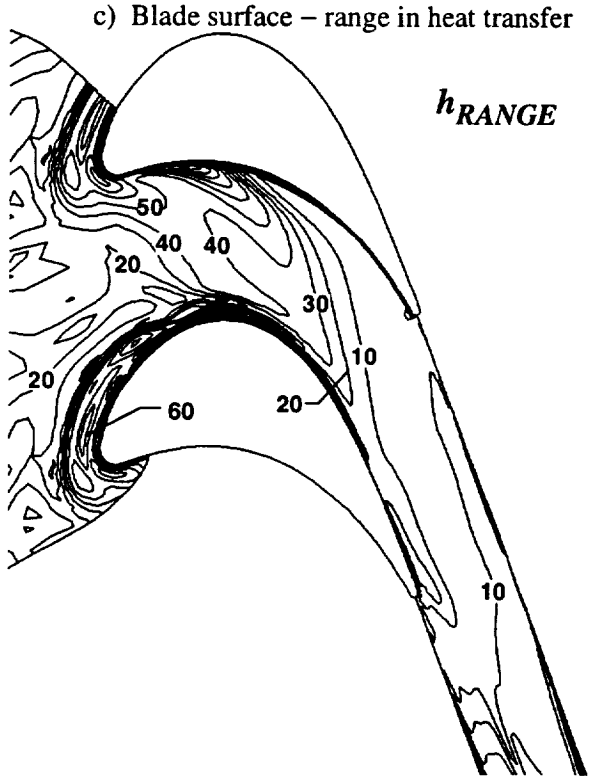

d) Hub endwall – range in heat transfer

Fig. 10 – Effect of not averaging stator exit flow field on rotor surface heat transfer. Uniform stator inlet temperature profile.

Chordwise hub surface heat transfer gradients upstream of the leading edge result from assuming endwall surface rotation started $0.20c_x$ upstream of the leading edge. Upstream of this location the hub surface was stationary. Because of the high inlet velocity, there is a region of very high heat transfer in front of the rotor. For most of the passage region the heat transfer is fairly uniform.

Figure 10 compares the local heat transfer obtained by averaging the results of three calculations with the tangentially averaged result for the uniform stator inlet temperature case. Three calculations were done using the stator exit

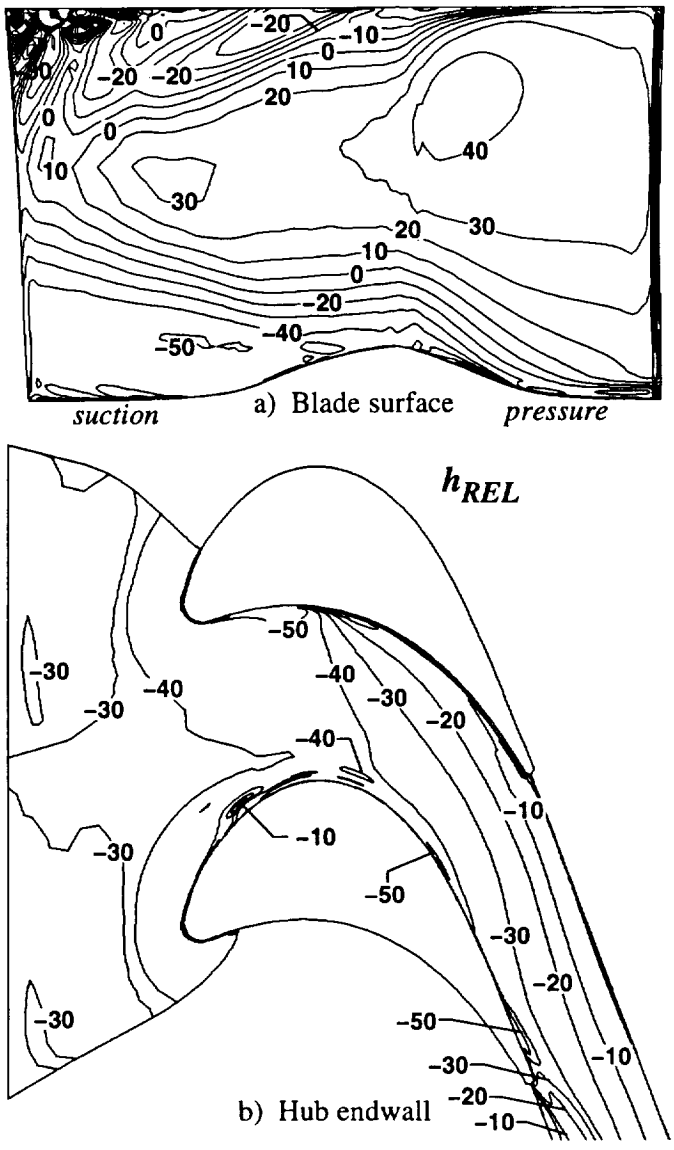

Fig. 11 Rotor heat transfer distribution – radial profile relative to uniform stator inlet profile. Tangentially averaged results.

profile shown in figure 8a positioned at different rotor inlet locations. The largest increase in rotor heat transfer is beyond midspan on the pressure surface. The increase exceeds 20%. The difference in hub heat transfer for the two approaches for calculating rotor heat transfer is small.

The range in surface heat transfer resulting from positioning the stator exit flow field at different rotor inlet locations is also shown in figure 10. The range in heat transfer can be thought of as the variation in heat transfer due to the position of the stator wake at the rotor inlet. Although not shown, there is an accompanying range in surface pressures resulting from the varying stator wake positions. The results show the range in heat transfer due to the rotor seeing the stator wakes at different locations. However, they may not completely represent the range in rotor heat transfer due to rotor-stator interactions, since unsteady effects are not accounted for. The rotor surface range in heat transfer is, as would be expected, large at the leading edge. Along the pressure surface the range is largest near the tip. The range is highest near the leading edge, and decreases in the chordwise direction. Along the suction surface the range decreases going from the leading to trailing edge. In the suction surface tip region there are again large gradients for the range in heat transfer. Because the suction surface tip region shows high gradients in heat transfer for all cases, the values for the range in this region should be treated with caution. Smoothing of the range values in this region is probably appropriate. The endwall heat transfer shows trends similar to those of the rotor blade. Near the leading edge, and close to the pressure surface, the range values are highest and decrease through the passage.

Relative heat transfer for the radial inlet case is shown in figure 11. Heat transfer obtained using the radially varying stator inlet total temperature profile shown in figure 3 is compared with the uniform stator inlet temperature profile heat transfer. For the comparisons the stator exit flow variables were averaged in the tangential direction. The midspan region experiences the full increase in heat transfer due to the increase in midspan driving potential. The only region that shows a significant reduction in heat load is the rear part of the suction surface blow midspan. Overall, there is a general increase in rotor heat load due to the stator inlet radial temperature distribution.

As expected, the hub endwall heat transfer decreases with a radial inlet temperature distribution. The average decrease in heat load is between 30 and 40%. These values are close to the increase in midspan driving potential for the radially varying case. It should be noted that the heat load for the radially varying case approaches the uniform inlet temperature case close to the pressure surface. Secondary flows result in higher temperature midspan fluid flowing down the pressure surface and across the hub endwall.

Figure 12 shows comparisons with experimental data. The predictions use the tangentially averaged stator exit conditions as input for the rotor analysis for both the uniform and radial stator inlet temperature profiles. Here the Nusselt number is defined as was done for the experimental data. $Nu = q_{WALL} c_x / k(T_{WALL})/(T''_{ROTOR-IN} - T_{WALL})$. The temperature difference is now based on rotor relative total temperature. For both the uniform and radially varying stator inlet temperature cases the analysis underpredicts the rotor heat load. The largest underprediction occurs along the forward part of the pressure surface. The results in figure 10 show that, if the average of individual rotor inlet cases was used to determine the rotor heat transfer, the agreement with

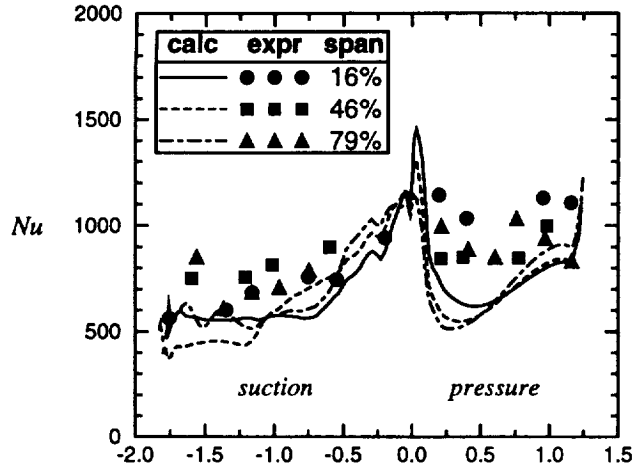

a) Uniform stator inlet temperature

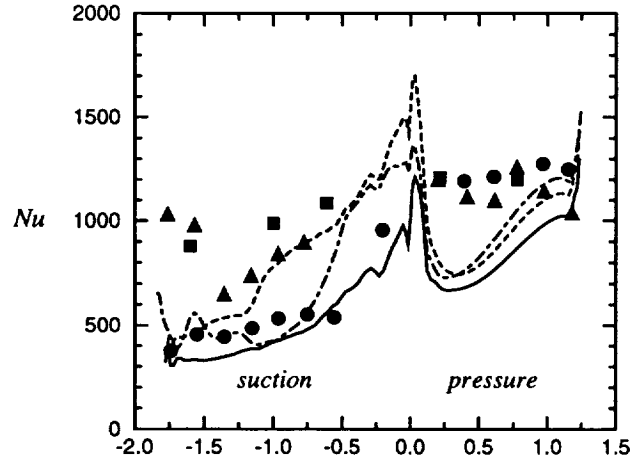

b) Radially varying stator inlet temperature

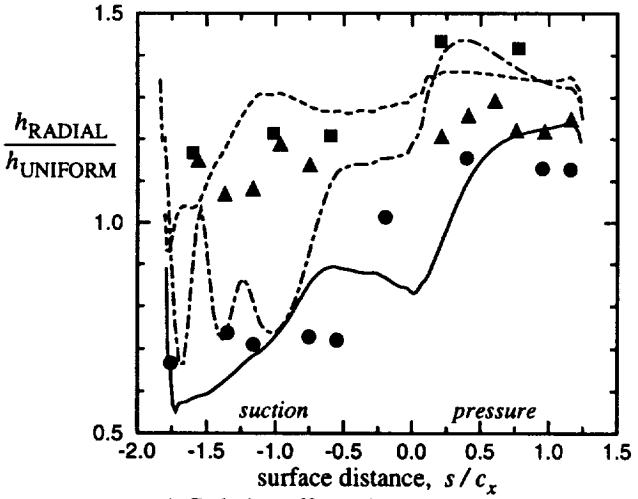

c) Relative effects due to radial variation

Fig. 12 Comparison with the data of Shang et al. (1996) for the effect of radially varying stator inlet temperature profile.

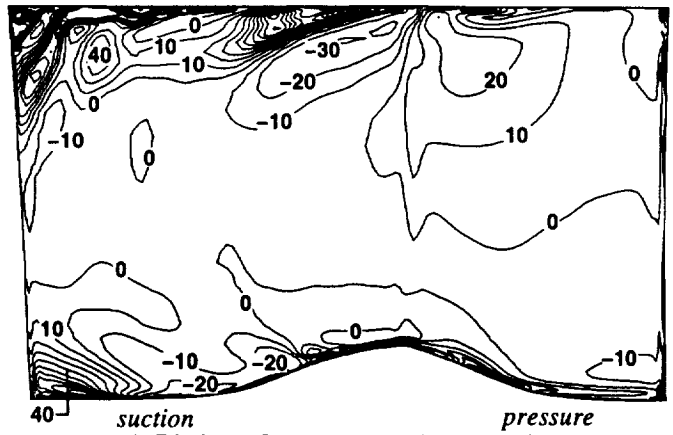

a) Blade surface – average heat transfer

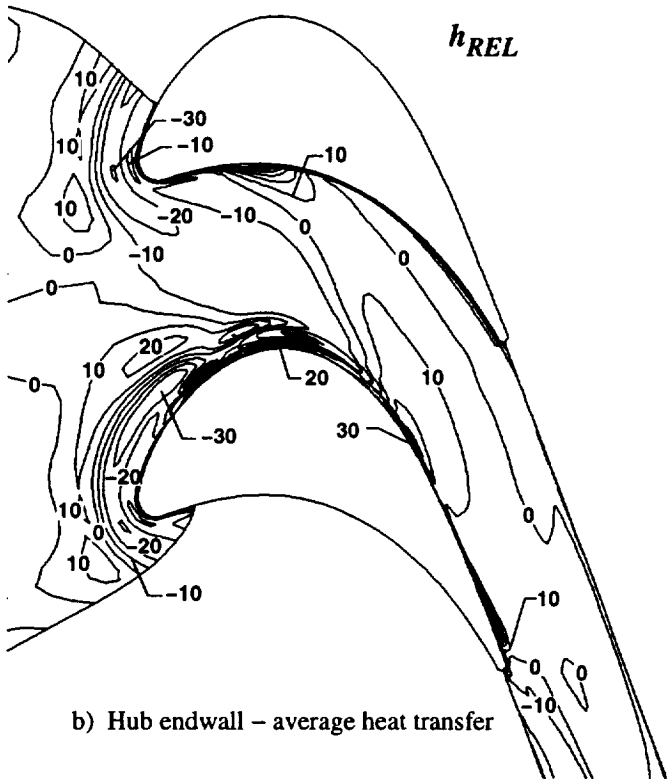

b) Hub endwall – average heat transfer

Fig. 13

the pressure surface data would improve. For the rear part of the suction surface the analysis underpredicts the heat transfer at 79% of span. Figure 9 shows this to be in a region of very rapidly changing heat transfer, and small changes in surface position can affect the agreement. Calculations at 85% of span show good agreement with the experimental data at 79% of span. Figure 12c shows that the ratio of surface heat transfer with a varying inlet profile to the heat transfer with a uniform inlet profile agrees reasonably well with the experimental data.

Next the question of how much the local rotor heat transfer is changed by assuming a tangentially averaged profile is addressed. Figure 10 showed the effects of a tangentially

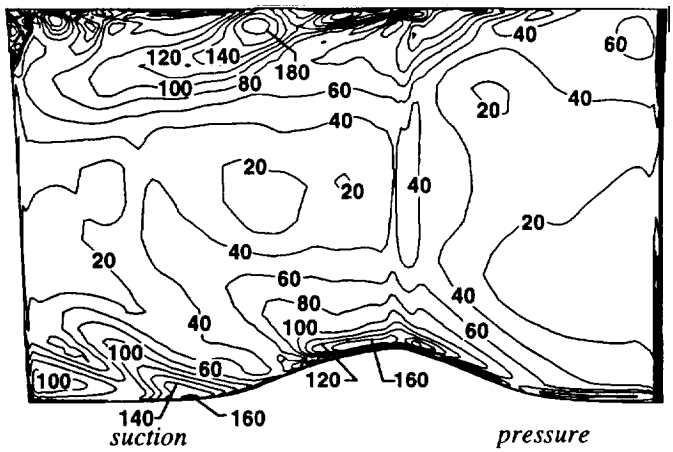

c) Blade surface – range in heat transfer

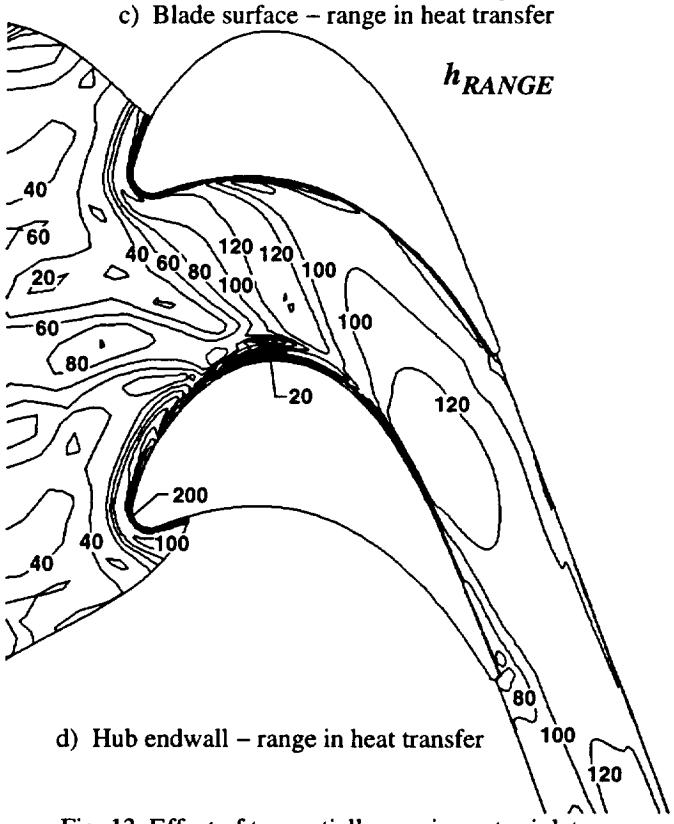

d) Hub endwall – range in heat transfer

Fig. 13 Effect of tangentially varying rotor inlet conditions on surface heat transfer. Radial stator inlet temperature profile.

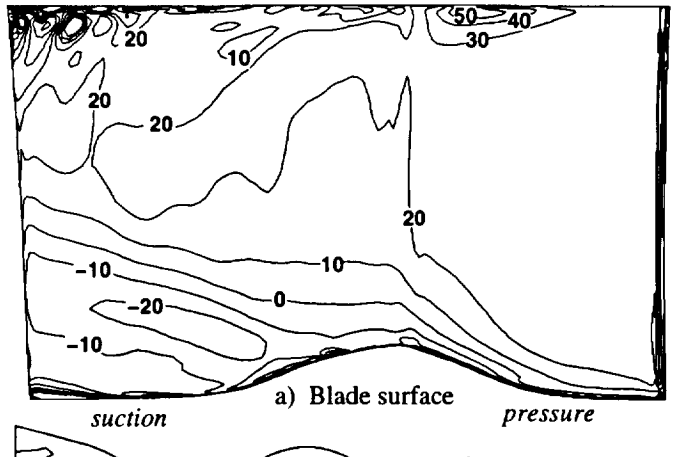

a) Blade surface

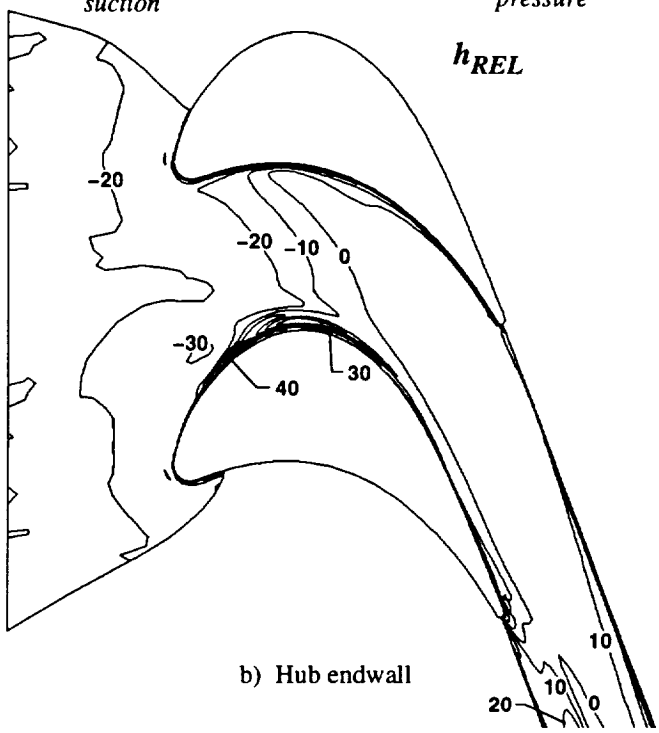

b) Hub endwall

Fig. 14 Average rotor heat transfer for tangentially varying stator inlet temperature profile relative to uniform stator inlet profile.

nonuniform rotor inlet flow field on the rotor average heat transfer and the range in heat transfer seen by the rotor. Figure 13 presents the same comparisons as figure 10, but for the case with a radial stator inlet temperature profile. Figure 13 shows the effect of not averaging the stator exit flow field in the tangential direction on surface heat transfer. The rotor average heat transfer and range in heat transfer with a radially varying stator inlet profile show the same behavior as the uniform stator inlet temperature profile case. The increase in hub heat transfer is nearly the same as for the uniform stator inlet temperature profile case. However, the range in heat transfer is considerably greater. This is not unexpected, since the hub heat transfer level is considerably less for the radially varying stator inlet temperature case.

The last question to be addressed is whether the local rotor surface heat transfer is affected by a tangential variation in the stator inlet temperature profile. Figure 8 showed different degrees of distortion at the stator exit depending on the location of the peak total inlet temperature relative to the stator leading edge. Figure 14 shows the ratio of the average heat transfer for all tangentially varying stator inlet total temperature cases to the uniform inlet temperature heat transfer. The reference case for this comparison is not the uniform stator inlet case with the flow field averaged in the tangential direction. The reference case in this figure is

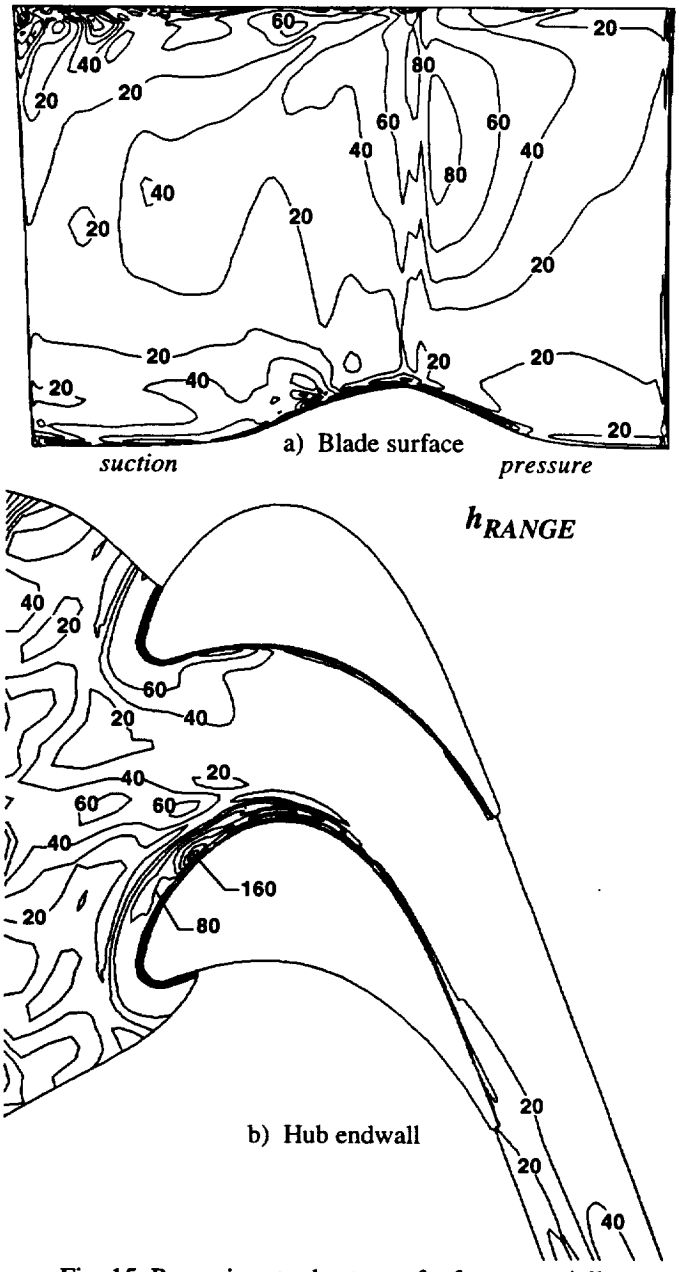

Fig. 15 Range in rotor heat transfer for tangentially varying stator inlet temperature profile.

the average of the calculations made for the stator wake in three rotor inlet locations. The reference case is the rotor heat transfer for the uniform stator inlet temperature profile. The average heat transfer for a stator inlet tangential temperature variation was determined from twelve cases. The twelve cases come from four locations of the stator inlet peak total temperature, and each profile's stator exit distribution at three rotor inlet locations. The rear portion of the pressure surface is higher by about 20% for the variation in stator inlet profile. This is consistent with the segregation of hot and cold fluid within the rotor measured by Butler et al. (1986).

For the nonuniform cases the suction surface heat load is higher above midspan, but lower below midspan. This could be the result of flow through the clearance gap from the pressure to suction surfaces. On the hub surface the heat load is unaffected by the stator inlet temperature variation, except near the rotor leading edge plane.

Figure 15 shows the heat transfer range for the tangentially varying case. On the blade surface the range is about the same as shown in figure 9 for the uniform stator inlet case. On the hub endwall the range is somewhat higher than for the uniform inlet case.

CONCLUDING REMARKS

Radial temperature profiles typical of those at a combustor exit resulted in decreased heat transfer on the stator and increased heat transfer on the rotor. As expected, the radial temperature variation reduced the heat load on the stator endwalls, and on the vane surface close to the endwalls. The increase in midspan heat load was less than would be calculated assuming that the heat load is proportional to the increase in gas-to-wall temperature difference.

Tangentially varying stator inlet profiles showed that the average stator heat load is only slightly affected by the tangential variation. However, the range in heat transfer indicated that a vane directly in front of a combustor inlet hot spot is likely to see a heat load increase proportional to the thermal driving potential. For the vane endwall the largest increase in heat load due to a combustor exit hot spot was in the forward part of the passage.

The rotor heat transfer due to positioning a wake at different locations in the rotor inlet plane was determined. These results were compared with the heat transfer calculated by averaging the stator exit flow field in the tangential direction. The principal change was higher heat transfer on the pressure surface for the average of individual calculations. This result is consistent with the segregation of hot and cold fluid as measured by Butler et al.(1986).

Overall there was a slight increase in rotor surface heat transfer for the radial variation in temperature case. However, there were large increases in rotor heat transfer for the pressure surface of the rotor. These results were consistent with the experimental measurements of Shang et al.(1996), and were again consistent with segregation of hot and cold fluid in the rotor as measured by Butler et al.(1986).

The approach taken in this analysis in which an inherently unsteady phenomena was modeled in a quasi-steady manner resulted in an envelope of heat load for the rotor. Future work would be to investigate whether this envelope is a reasonable estimate of the envelope of rotor heat transfer seen by actual rotors.

Results were shown for one stage at one operating point. The approach used accurately predicted the change in rotor

heat transfer due to a stator inlet radial temperature variation. Those results which are significant from a design point should be verified by comparisons with experimental data. Doing so would increase confidence in this approach to predicting both the effects of combustor exit temperature variations on blade row heat transfer, and the range in heat transfer due to rotor inlet tangential nonuniformities. The calculated range in heat transfer, and the accompanying range in surface pressures should be compared with experimental data to determine if the results provide an approximation for unsteady effects.

Acknowledgements

Computational resources were provided by the NASA NAS facility at the Ames Research Center.

REFERENCES

Ameri, A.A. and Steinthorsson E., 1995, "Prediction of Unshrouded Rotor Blade Tip Heat Transfer," ASME paper 95-GT-142.

Ameri, A.A. and Arnone, A., 1994, "Prediction of Turbine Blade Passage Heat Transfer Using a Zero and a Two-Equation Turbulent Model," ASME Paper 94-GT-122.

Arnone, A., and Pacciani, R., 1996, "Rotor-Stator Interaction Analysis Using the Navier-Stokes Equations and a Multigrid Method," ASME *Journal of Turbomachinery*, Vol. 118, No. 4, pp. 679-689.

Arnone, A., Liou, M.-S., and Povinelli, L. A., 1992, "Navier- Stokes Solution of Transonic Cascade Flows Using Non-Periodic C-Type Grids," AIAA *Journal of Propulsion and Power*, Vol. 8, No. 2, pp. 410-417.

Baldwin, B.S. and Lomax, H., 1978, "Thin-Layer Approximation and Algebraic Model for Separated Turbulent Flows," AIAA Paper AIAA-78-257.

Boyle, R.J., and Lucci, B.L., 1996,"Predicted Turbine Heat Transfer For a Range of Test Conditions," ASME paper 96-GT-304.

Boyle, R.J, and Jackson, R., 1995,"Heat Transfer Predictions for Two Turbine Nozzle Geometries at High Reynolds and Mach Numbers," ASME paper 95-GT-104.

Boyle, R.J., and Giel, P.W., 1995, "Three-Dimensional Navier-Stokes Heat Transfer Predictions for Turbine Blade Rows," AIAA *Journal of Propulsion and Power*, Vol. 11, No. 6, pp. 1179-1186.

Butler, T.L., Sharma, O.P., Joslyn, H.D., and Dring, R.P., 1986, "Redistribution of an Inlet Temperature Distortion in an Axial Flow Turbine Stage," AIAA paper 86-1486.

Chima, R.V., and Yokota, J.W., 1988, "Numerical Analysis of Three-Dimensional Viscous Internal Flows," AIAA paper 88-3522, (NASA TM-100878).

Chima, R.V., 1991, "Viscous Three-Dimensional Calculations of Transonic Fan Performance," AGARD Propulsion and Energetics Symposium on Computational Fluid Mechanics for Propulsion, San Antonio, Texas, May 27-31.

Chima, R.V., Giel, P.W., and Boyle, R.J., 1993, "An Algebraic Turbulence Model for Three-Dimensional Viscous Flows," AAIA paper 93-0083, (NASA TM-105931).

Chima, R.V., 1996, "Application of the $k-\omega$ Turbulence Model to Quasi-Three-Dimensional Turbomachinery Flows," AIAA *Journal of Propulsion and Power*, Vol. 12, No. 6, pp. 1176-1179.

Cox, G.B., 1975, "An Analytic Model for Predicting Exit Temperature Profile From Gas Turbine Engine Annular Combustors," AIAA paper 75-1307.

Crocker, D.S., Smith, C.E., and Myers, G.D., 1994, "Pattern Factor Reduction in a Reverse Flow Gas Turbine Combustor Using Angled Dilution Jets," ASME paper 94-GT-406.

Davis, R.L., Shang, T., Buteau, J. and Ni, R.H., 1996, "Prediction of 3-D Unsteady Flow in a Multi-Stage Turbomachinery Using an Implicit Dual Time-Step Approach," AIAA paper 96-2565.

Dorney, D.J., Davis, R.L., and Sharma, O.P., 1996, "Unsteady Multistatge Analysis Using a Loosely Coupled Blade Row Approach," AIAA *Journal of Propulsion and Power*, Vol. 12, No. 2, pp. 274-282.

Heselhaus, A., and Vogel, D.T., 1995, "Numerical Simulation of Turbine Blade Cooling with Respect to Blade Heat Conduction and Inlet Temperature Profiles," AIAA paper 95-3041.

Jorgenson, P.C.E., and Chima, R.V., 1988, "An Explicit Runge-Kutta Method for Unsteady Rotor/Stator Interactions," AIAA paper 88-0049.

Mayle, R.E., 1991, "The Role of Laminar-Turbulent Transition in Gas Turbine Engines," ASME *Journal of Turbomachinery*, Vol. 113, pp. 509-537.

Rao, K.V., Delaney, R.A., and Dunn, M.G., 1992, "Vane-Blade Interaction in a Transonic Turbine Part I-Aerodynamics," AIAA paper 92-3323.

Rao, K.V., Delaney, R.A., and Dunn, M.G., 1992a,"Vane-Blade Interaction in a Transonic Turbine Part II-Heat Transfer," AIAA paper 92-3324.

Saxer, A.P., and Giles, M.B., 1990, "Inlet Radial Temperature Redistribution in a Transonic Turbine Stage," AIAA paper 90-1543.

Shang, T., Guenette, G.R., Epstein, A.H. and Saxer, A.P., 1995, "The Influence of Inlet Temperature Distortion on Rotor Heat Transfer in a Transonic Turbine," AIAA paper 95-3042.

Sorenson, R.L., 1980, "A Computer Program to Generate Two-Dimensional Grids About Airfoils and Other Shapes by the Use of Poisson's Equation," NASA TM 81198.

Suo, M., 1985, "Turbine Cooling," in *Aerothermodynamics of Aircraft Engine Components*, G.C. Oates editor, Amer-

ican Institute of Aeronautics and Astronautics, Inc. publisher.

Takahashi, R., and Ni, R.H., 1991, "Unsteady Hot Streak Simulation Through 1-1/2 Stage Turbine," AIAA paper 91-3382.

REPORT DOCUMENTATION PAGE

Form Approved
OMB No. 0704-0188

1. AGENCY USE ONLY (*Leave blank*)	2. REPORT DATE	3. REPORT TYPE AND DATES COVERED
	September 1997	Technical Memorandum

4. TITLE AND SUBTITLE

Prediction of Nonuniform Inlet Temperature Effects on Vane and Rotor Heat Transfer

5. FUNDING NUMBERS

WU-523-26-13

6. AUTHOR(S)

Robert J. Boyle and Paul W. Giel

7. PERFORMING ORGANIZATION NAME(S) AND ADDRESS(ES)

National Aeronautics and Space Administration
Lewis Research Center
Cleveland, Ohio 44135-3191

8. PERFORMING ORGANIZATION REPORT NUMBER

E-10862

9. SPONSORING/MONITORING AGENCY NAME(S) AND ADDRESS(ES)

National Aeronautics and Space Administration
Washington, DC 20546-0001

10. SPONSORING/MONITORING AGENCY REPORT NUMBER

NASA TM-107539
ASME-97-GT-133

11. SUPPLEMENTARY NOTES

Prepared for the Turbo-Expo 1997 sponsored by the International Gas Turbine Institute of the American Society of Mechanical Engineers, Orlando, Florida, June 2–5, 1997. Robert J. Boyle, NASA Lewis Research Center and Paul W. Giel, NYMA, Inc., Brook Park, Ohio. Responsible person, Robert J. Boyle, organization code 5820, (216) 433–5889.

12a. DISTRIBUTION/AVAILABILITY STATEMENT

Unclassified - Unlimited
Subject Category 34

This publication is available from the NASA Center for AeroSpace Information, (301) 621–0390.

12b. DISTRIBUTION CODE

13. ABSTRACT ***(Maximum 200 words)***

The effects of nonuniform combustor exit temperature profiles on vane and rotor heat transfer were determined using a steady-state three-dimensional Navier-Stokes analysis. Both radial and tangential nonuniform temperature profiles were individually considered. Comparisons are made with experimental data for the effects of a radial temperature nonuniformity on rotor heat transfer. There was a decrease in stator heat load, and an increase in rotor heat load for a radial temperature distribution typically seen at the combustor exit. Tangential variations in stator inlet temperature produced significant variations in stator heat load, and resulted in average rotor heat load greater than for the uniform inlet temperature case. Rotor heat load was also calculated for different stator wake locations. Accounting for the stator wake position at the rotor inlet gave a greater average rotor heat load than that obtained by averaging the stator exit flow field in the tangential direction. The increase was most notable on the rotor pressure surface.

14. SUBJECT TERMS	15. NUMBER OF PAGES
Gas turbine; Heat transfer; Navier-Stokes	18
	16. PRICE CODE: A03

17. SECURITY CLASSIFICATION OF REPORT	18. SECURITY CLASSIFICATION OF THIS PAGE	19. SECURITY CLASSIFICATION OF ABSTRACT	20. LIMITATION OF ABSTRACT
Unclassified	Unclassified	Unclassified	